Notes on the OWA Yagi

Wouldn't you like a high-performance wide-bandwidth antenna? An Optimized Wideband Antenna (OWA) Yagi may be the answer. Come learn a little about how OWAs work and what potential they hold.

By L. B. Cebik, W4RNL

Perhaps the most-read source of information on the "Optimized Wideband Antenna (OWA) Yagi" comes from a series of Web site entries by Nathan Miller, NW3Z, and Jim Breakall, WA3FET (**nw3z.contesting.com**). Besides providing a very brief background for the design features of the OWA Yagi, the articles present specific designs for the upper HF bands used in contests.

According to the OWA account, when we place a parasitic element close (less than 0.01 wavelength) ahead of a driven element, we obtain wide-band performance. That is, we get a low SWR relative to 50 Ω, smooth gain and front-to-back performance over a wide HF amateur band (such as 20, 15 or 10 meters). The authors suggest that the driver and first director perform as if they were a single element having a diameter equal to the spacing between the two elements.

Extensive *NEC-4* modeling studies of the actual OWA designs suggest that we may need an expanded account of how these antennas work. As well, these modeling investigations also suggest some unanticipated benefits of OWA design in antennas larger than the typical six-element HF design. To demonstrate these suggestions, I have transferred the OWA design to two meters, where full coverage of 144-148 MHz is often a challenge. The band exhibits a 2.7% bandwidth relative to its center frequency (146 MHz), which is wider than most of the HF bands from 20 meters on up, with the exception of 10 meters, which has a bandwidth of about 3.5%. We shall look briefly in these proceedings at even wider bandwidths.

As well, modeling the antennas at two meters permits the use of uniform-diameter elements. These elements allow simplified models, from the standpoints of both optimizing a design and reading the results. All of the models that we shall selectively survey will presume elements that are well insulated and isolated from any conductive support boom. Several of the designs have been successfully built, with performance meeting the modeled expectations.

Modeling permits us to view the cur-

1434 High Mesa Dr
Knoxville, TN 37938-4443
cebik@cebik.com

rent magnitude and phase angle on each element (using the element center) relative to the source or feed-point current. The current data provides important clues in our search for an expanded understanding of OWA operation. The downside of the investigation technique is that our presentation will be heavily laden with graphs and tables.

Despite an appearance of extensive investigation, this study is incomplete. It samples only a few of the many OWA designs in my stock, and even if they seem typical, I cannot make a claim of complete coverage. Hence, the conclusions are only suggestive, but not in any way authoritative. If past Yagi developments teach anything, it is that something new lies ahead in the development of parasitic arrays.

Introduction to a Six-Element 2-Meter OWA Yagi

We shall begin with the six-element, two-meter OWA Yagi whose outline appears in Fig 1, with dimensions shown in Table 1. The sketch provides the traditional element designations, which include a single reflector, a single driver and four directors. However, before we are finished with this beam, we shall have occasion to rethink our element designations. The design is an adaptation of an NW3Z/WA3FET 20-meter design.

The dimensions in Table 1 should arouse our interest. I have given them in inches and wavelengths for convenience. The first director is 0.052 λ from the driver, in accord with the general OWA design precepts.

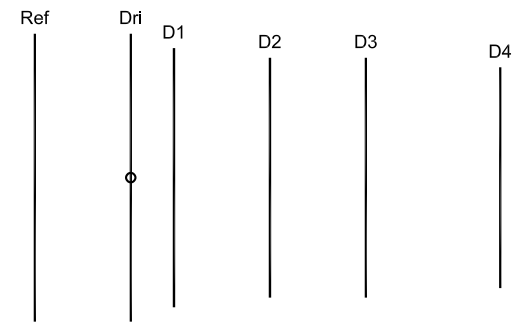

Fig 1—An outline sketch of a six-element OWA Yagi, showing the traditional element designations. Model OWA2M616: see Table 1 for dimensions.

Table 1—Model OWA2M616 Dimensions

Dimensions of a 6-element 2-meter OWA Yagi using 0.1875" ($^3/_{16}$") diameter elements. Wavelength (λ) measurements are for a design center frequency of 146 MHz.

	Length		*Cumulative Spacing*		*Individual Spacing*	
Element	*Inches*	*λ*	*Inches*	*λ*	*Inches*	*λ*
Refl	40.52	0.501	—	—	—	—
Driver	39.96	0.494	10.13	0.125	10.13	0.125
Dir 1	37.38	0.462	14.32	0.177	4.19	0.052
Dir 2	36.31	0.449	25.93	0.321	11.61	0.144
Dir 3	36.31	0.449	37.28	0.461	11.35	0.140
Dir 4	34.96	0.433	54.22	0.671	16.94	0.210

Table 2—6-Element 2-Meter OWA Yagi

NEC-4 reported performance data for model OWA2M616 from 139 to 149 MHz. Current data consist of the relative current magnitude and phase angle on the center segment of each element, where the driver current magnitude is always 1.0 and the driver phase angle is always 0.0°. The "D2 versus D3 currents" consist of the ratio of current magnitude from Director 2 to Director 3 and of the current phase-angle difference between the two directors. (See text for data interpretation.)

Performance											
Frequency (MHz)	*139*	*140*	*141*	*142*	*143*	*144*	*145*	*146*	*147*	*148*	*149*
Free Space Gain (dBi)	9.38	9.68	9.86	9.97	10.06	10.13	10.19	10.23	10.23	10.16	10.01
180° F/B (dB)	8.34	10.61	12.9	15.35	18.23	22.04	28.2	35.39	26.71	22.17	20
R (Ω)	27.85	32.99	37.33	40.51	42.78	44.79	47.18	49.97	50.82	43.6	27.9
X (Ω)	–8.58	–3.56	–0.1	2.56	5.07	7.61	9.62	9.52	5.18	–1.719	–0.98
SWR (50 Ω)	1.871	1.529	1.34	1.244	1.21	1.215	1.229	1.21	1.109	1.152	1.793
Currents											
Ref-Magnitude	0.805	0.764	0.708	0.647	0.588	0.54	0.503	0.472	0.428	0.34	0.208
Ref-Phase (°)	147.5	138.36	130.1	123.08	117.28	112.2	106.78	99.29	87.69	71.67	57.19
D1-Magnitude	0.492	0.592	0.686	0.771	0.856	0.952	1.079	1.257	1.481	1.657	1.641
D1-Phase (°)	–76.11	–80.96	–86.43	–91.64	–96.19	–100.1	–104.1	–109.5	–118.6	–132.8	–148.4
D2-Magnitude	0.369	0.437	0.5	0.558	0.613	0.67	0.733	0.799	0.845	0.809	0.655
D2-Phase (°)	233.1	224.3	214.8	205.1	195.4	185.5	174.69	161.83	145.43	125.6	107.83
D3-Magnitude	0.34	0.403	0.462	0.52	0.58	0.649	0.735	0.844	0.962	1.02	0.949
D3-Phase (°)	174.94	164.96	154.44	143.9	133.48	122.87	111.43	97.47	79.44	56.65	33.21
D4-Magnitude	0.301	0.357	0.41	0.459	0.508	0.561	0.623	0.696	0.763	0.769	0.67
D4-Phase (°)	92.97	80.21	66.75	53.06	39.26	25.02	9.58	–8.47	–30.94	–58.41	–86.67
D2 versus D3 Currents											
Magnitude Ratio	1.085	1.084	1.082	1.073	1.057	1.032	0.997	0.947	0.878	0.793	0.69
Phase Difference (°)	58.16	59.34	60.66	61.2	61.92	62.63	63.35	64.36	65.99	68.95	74.62

However, note the lengths of directors D2 and D3: They are identical. (In actuality, OWA designs of this type may use a third director that is slightly shorter or slightly longer—by up to about 1%—than director 2, according to overall design goals.) The lengths of these two directors are no accident, even if their role in the OWA design is often overlooked.

There is often a vast difference between the exceptionally wide 50-Ω SWR curve of an OWA design and the intended operating bandwidth of the antenna. Table 2 presents the modeled characteristics of this six-element Yagi from 139 to 149 MHz, although the performance characteristics focus on the 144-148-MHz span. The design goals use typical Amateur Radio guidelines for the 0.67-λ boom: a free-space gain of at least 10 dBi, a 180° and worst-case front-to-back ratio of at least 20 dB and as flat a 50-Ω SWR as we may achieve. Fig 2 shows that the antenna easily meets the gain and front-to-back guidelines from 144 to 148 MHz.

Fig 3 presents the 50-Ω SWR curve for the array from 139 to 149 MHz. The curve is typical of optimized OWA designs. Yes, even an optimized broadband antenna may be optimized within its overall design parameters. Most noticeable and telling is the presence of two dips in the SWR, one shallow dip at 143 MHz and one very sharp dip near 147.5 MHz. The rise in SWR above 148 MHz is very steep, while below the operating passband for the antenna, the SWR rises very slowly.

The graph of resistance and reactance across the entire scanned spectrum, Fig 4, shows us why the SWR remains so flat. The feed-point resistance and reactance both vary across an extremely small range, with the largest incremental changes occurring above the operating passband. The reactance begins as a small capacitive value, changes to a set of inductive values, and returns to capacitive values at the high end of the scanned passband. We might miss these patterns if we look only within the operating passband for the antenna.

Most OWA designs place the operating passband near the upper end of the SWR passband. In this region, we usually find the lowest SWR value in conjunction with the flattest curve at the lower end of the impedance passband. However, the steep rise in SWR above the operating passband requires significant care in array construction to avoid moving the SWR curve into the region of rapid change. In fact, nothing dictates that the operating passband must be in this region. Indeed, with lesser levels of gain and front-to-

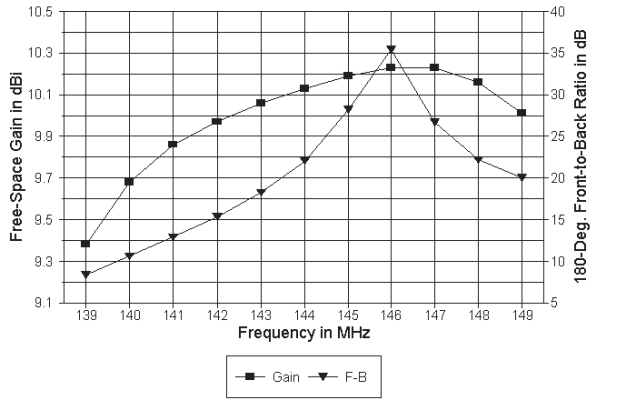

Fig 2—The modeled free-space gain and 180° front-to-back performance of Model OWA2M616 from 139 to 149 MHz. See Table 2 for numeric data.

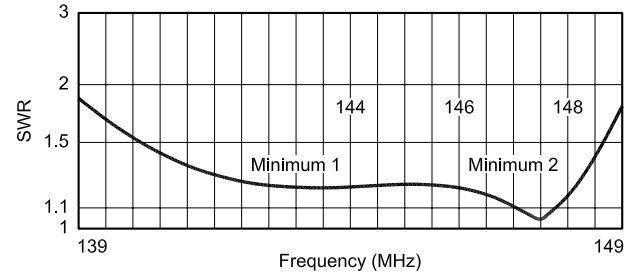

Fig 3—50-Ω SWR curve for model OWA2M616 from 139 to 149 MHz.

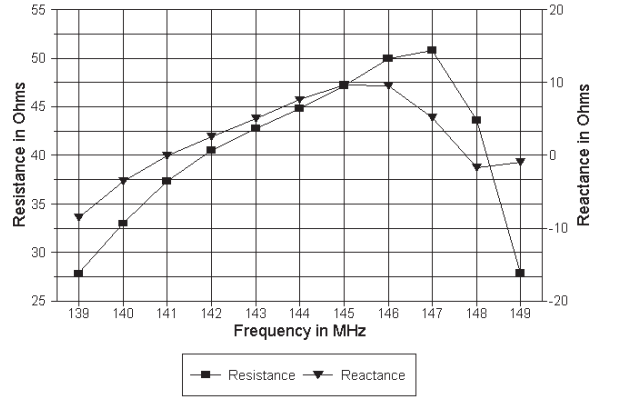

Fig 4—Feed-point resistance and reactance for model OWA2M616 from 139 to 149 MHz.

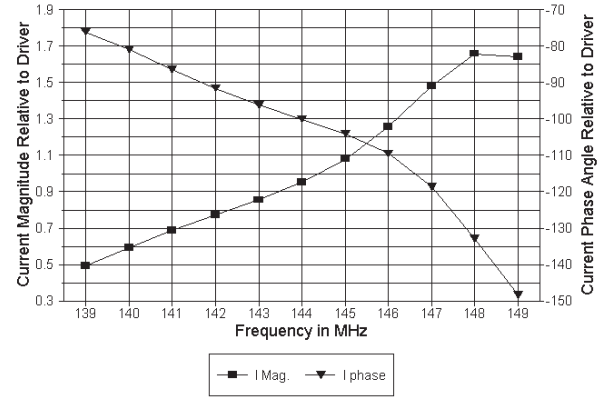

Fig 5—The current magnitude and phase angle on director 1 of model OWA2M616 from 139 to 149 MHz relative to a value of 1.0 and 0.0° on the center segment of the driven element.

back ratio, we may spread the operating region across most of the low SWR region. Moreover, the width of the "low" SWR region is limited mostly by the level to which we are willing to allow the SWR to rise between the minima. Most, but not all, extant OWA designs try to keep the mid-region values as low as feasible.

Designing an OWA Yagi, then, is a balance between the operating specifications (and possibilities for a given boom length) on the one hand and the desired SWR level and curve on the other. Changing one or the other set of specifications will alter the resulting physical design. Hence, there can be no "ultimate" OWA design. However, with a given set of operating and SWR specifications, we can try to see how the OWA achieves its goals.

OWA-1: Understanding the OWA with Reference to the Reflector, Driver and First Director

The initial perspective that we shall take on the OWA follows the received account of its operation. The spacing between the driver and the first director sets the 50-Ω SWR curve for the array. Of course, the length and spacing of the reflector play a significant role in establishing the reference impedance for the SWR curve—in addition to playing a smaller role in setting the operational band-edge performance of the array.

With this perspective applied to our initial six-element OWA Yagi, we find a reflector about $^1/_8$-λ behind the driver, with the first director spaced about 0.052-λ ahead. If we set the driver current magnitude to a value of 1.0 and a phase angle of 0.0° for every scanned frequency, we may track the relative current magnitude and phase angle on the first (close-spaced) director. Fig 5 shows the results of this exercise.

As expected, the first director shows a negative current phase angle relative to the driver. However, note that the curve steepens, indicating a greater rate of change above about 146 MHz. At the same time, the current magnitude on the first director continuously increases with rising frequency—until we reach 148 MHz. The current magnitude is actually greater on the first director than on the driver from 145 MHz upward.

In effect, the driver and first director actually form a primary (fed) driver and secondary (parasitic) driver pair. (When applied to different frequency bands, the pair sometimes goes under the names master and slaved driver. However, for in-band applications, the terms primary and secondary may be more apt.) As the secondary driver becomes dominant, the rate of change of its current phase angle increases.

The question that remains is this: Is the account sufficient to set the OWA design apart as unique? If we limit our investigation only to the reflector/driver/first-director trio of elements, then the concept is not new, but only refined by the use of very close spacing of director 1 to the driver. For example, the DL6WU family of VHF/UHF Yagis uses 0.075-λ spacing for director 1 to obtain very wide-band operation for Yagis ranging from 6 to *n* elements. See Chapter 7 (by Gunter Hoch, DL6WU) of the RSGB publication, *The VHF/UHF DX Book*, edited by Ian White, G3SEK, for perhaps the last iteration of this classic set of Yagis. Experimental Yagi designs using "fat" elements have achieved operating bandwidths (including usable gain and front-to-back ratios) of greater than 23% of the central frequency of the passband.

At a more modest size—in fact, quite comparable in boom length to our six-element OWA Yagi—is an adaptation of a five-element broadband Yagi design that originated from the work of Jack Reeder, W6NGZ (now WW7JR), and that appears in *CQ* magazine of October, 1996. The design made no pretense about using OWA principles, but simply strove to cover 20 meters within the usual standards for good Amateur Radio performance. I have adapted the design to $^3/_{16}$-inch elements and two meters for comparison with the six-element OWA design.

Fig 6 shows the array outline for comparison with the OWA outline in Fig 1. Table 3 provides the dimensions, which show the boom length to be about $^3/_4$-inch shorter than the six-element OWA. However, there are only five elements. The reflector is about 0.123 λ behind the driver, with the first director 0.089 λ ahead.

Table 4 supplies a complete performance table comparable to the data in Table 2 for the six-element OWA Yagi. We can begin by comparing Fig 7 to Fig 2 to gauge the success of the five-element design in achieving the performance goals. In fact, the performance curves in the two figures have very similar shapes, with the smaller design having lower performance numbers at the scanning limits. From the table, you may determine that over the 144 to 148-MHz operating passband, the five-element Yagi misses the 20-dB front-to-back ratio guideline by an amount too small to make any difference.

The feed-point resistance and reac-

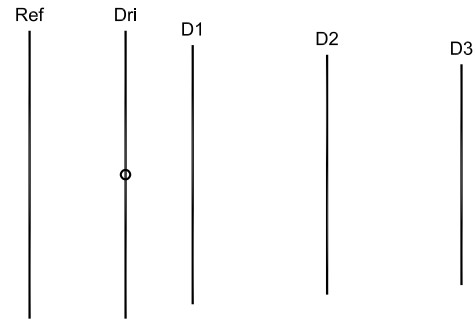

Fig 6—An outline sketch of a five-element wide-band Yagi, showing the traditional element designations. Model 2M5EL16: see Table 3 for dimensions.

Table 3—Model 2M5EL16 Dimensions

Dimensions of a 5-element 2-meter wide-band Yagi using 0.1875" ($^3/_{16}$") diameter elements. Wavelength (λ) measurements are for a design center frequency of 146 MHz.

Element	*Length*		*Cumulative Spacing*		*Individual Spacing*	
	Inches	*λ*	*Inches*	*λ*	*Inches*	*λ*
Refl	40.46	0.501	—	—	—	—
Driver	39.26	0.486	9.90	0.123	9.90	0.123
Dir 1	37.19	0.460	17.10	0.212	7.20	0.089
Dir 2	36.88	0.456	34.80	0.431	17.70	0.219
Dir 3	35.64	0.441	53.50	0.662	28.70	0.231

Table 4—5-Element 2-Meter Wide-Band Yagi

NEC-4 reported performance data for model 2M5EL16 from 139 to 149 MHz. Current data consist of the relative current magnitude and phase angle on the center segment of each element, where the driver current magnitude is always 1.0 and the driver phase angle is always 0.0°. The "D1 versus D2 currents" consist of the ratio of current magnitude from Director 1 to Director 2 and of the current phase angle difference between the two directors. (See text for data interpretation.)

Performance											
Frequency (MHz)	*139*	*140*	*141*	*142*	*143*	*144*	*145*	*146*	*147*	*148*	*149*
Free Space Gain (dBi)	9.29	9.62	9.81	9.94	10.05	10.16	10.26	10.33	10.32	10.15	9.69
180° F/B (dB)	7.02	9.18	11.53	13.65	16.37	20.11	26.75	41.94	24.47	19.73	18.23
R (Ω)	25.09	29.83	33.44	35.21	35.43	35.08	35.46	38.1	43.5	39.13	15.36
X (Ω)	–20.77	–15.5	–12.09	–9.41	–6.26	–1.99	3.23	8.02	7.52	–4.93	–1.75
SWR (50 Ω)	2.427	1.911	1.643	1.514	1.454	1.43	1.422	1.387	1.237	1.309	3.26
Currents											
Ref-Magnitude	0.818	0.77	0.699	0.618	0.542	0.484	0.45	0.438	0.426	0.319	0.099
REF-Phase (°)	152.42	143.2	135.02	128.74	124.83	123	121.82	118.4	107.48	83.68	80.34
D1-Magnitude	0.507	0.61	0.7	0.77	0.824	0.873	0.942	1.081	1.379	1.759	1.658
D1-Phase (°)	–78.73	–85.44	–93.02	–100.3	–106.3	–110.6	–112.9	–114.3	–119.4	–137.9	–161.6
D2-Magnitude	0.381	0.461	0.539	0.613	0.689	0.779	0.904	1.099	1.399	1.537	1.221
D2-Phase (°)	206.8	197.5	187.3	177.03	167.1	157.41	147.13	134.2	113.77	78.54	40.69
D3-Magnitude	0.316	0.379	0.437	0.487	0.531	0.579	0.641	0.734	0.869	0.91	0.623
D3-Phase (°)	108.7	95.73	81.74	67.54	53.54	39.65	25.09	7.86	–16.82	–56.15	–97.8
D1 versus D2 Current											
Magnitude Ratio	1.331	1.323	1.299	1.256	1.196	1.121	1.042	0.984	0.986	1.144	1.358
Phase Difference (°)	285.53	282.94	280.32	277.33	273.4	268.01	260.03	248.5	233.17	216.44	202.29

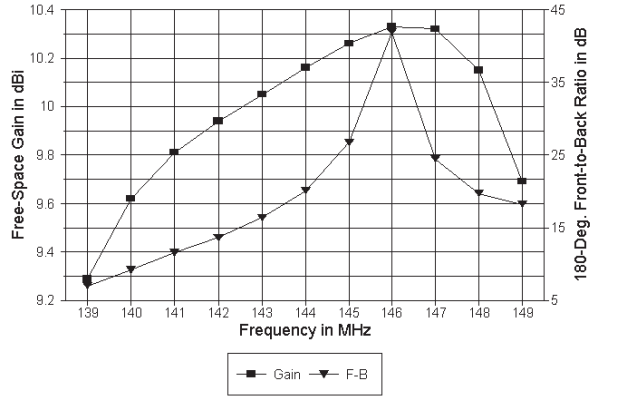

Fig 7—The modeled free-space gain and 180° front-to-back performance of Model 2M5EL16 from 139 to 149 MHz. See Table 2 for numeric data.

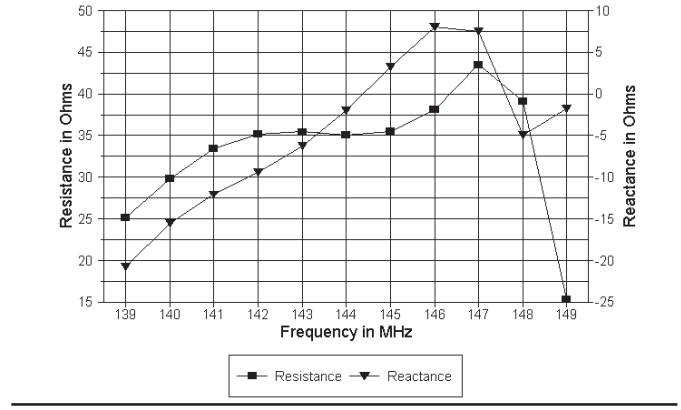

Fig 8—Feed-point resistance and reactance for model 2M5EL16 from 139 to 149 MHz.

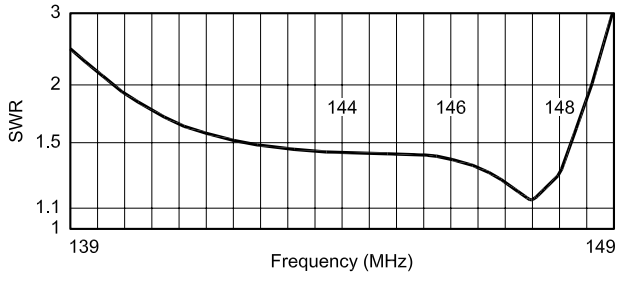

Fig 9—50-Ω SWR curve for model 2M5EL16 from 139 to 149 MHz.

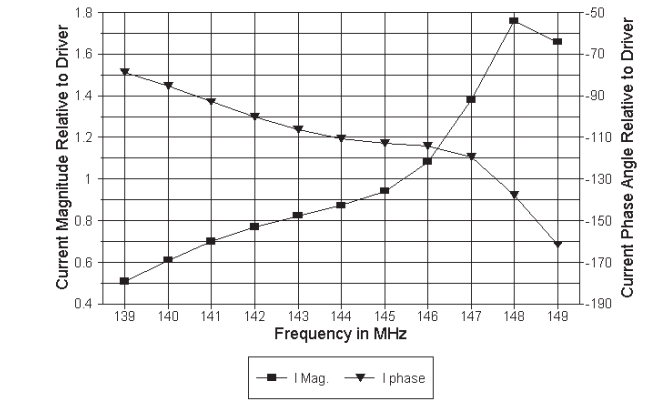

Fig 10—The current magnitude and phase angle on director 1 of model 2M5EL16 from 139 to 149 MHz relative to a value of 1.0 and 0.0° on the center segment of the driven element.

tance curves in Fig 8 also show considerable similarity to those for the OWA Yagi in Fig 4. The median resistance is in the 35 to 40-Ω range because of the spacing of the reflector from the driver. The original array for 20 meters was designed to a certain boom-length limit, so long as the 50-Ω SWR values remained below 2:1 within the operating passband. Fig 9 shows the five-element Yagi 50-Ω SWR curve. It exhibits the same general shape as Fig 3 for the OWA Yagi, but without a definite minimum within the lower frequency region of the span. Had we used a reference impedance of 35 to 40 Ω, the overall curve would have come closer to achieving better than 2:1 values across the scanned passband.

Like the six-element OWA Yagi, the first director functions as a secondary driver. Between 145 and 146 MHz, the current magnitude exceeds a ratio of 1.0:1 relative to the current magnitude on the primary driver, as shown in Fig 10. Indeed, allowing for the difference in curve shapes that is due to changes in the axis increments, the curves for both current magnitude and phase angle are remarkably similar. Only the current phase angle of the smaller array increases at a higher rate at the upper limit of the scanned frequency range.

An interesting facet of the wide-band five-element array appears in Fig 11, a graph of the differentials in current magnitude and phase angle between director 1 (the secondary driver) and director 2. The ratio of director 1 to director 2 current magnitude varies over a quite small range, much smaller than the current magnitude excursions for any other element pair in the array. The current phase-angle difference also remains relatively constant for nearly the full lower half of the scanned frequency range, decreasing ever more rapidly thereafter. In this upper portion of the frequency range, the secondary driver/first director becomes ever more dominant in driving the array.

In short, there is little in the reflector-driver-director-1 portion of the array to distinguish the six-element OWA Yagi from the five-element wide-band Yagi. Granted, the larger array has a measurably wider impedance bandwidth and slightly narrower boundaries to the range of impedance and current values sampled from 139 to 149 MHz. However, it does not appear that the reflector-driver-director-1 portion of the array is sufficient to account for the smoother performance of the OWA.

OWA-2: Understanding the OWA with Reference Also to the Second and Third Directors

Often overlooked are the second and third directors of the six-element OWA design. These elements are those having almost, if not actually, identical lengths. They show some interesting properties within the overall OWA structure.

A glance at Table 2 shows that the first and second directors of the OWA array do not present the same level of close correlation among the current numbers as the corresponding elements in the five-element Yagi. Indeed, it appears that the first director of the smaller beam does double duty relative to the OWA array with its extra element. The five-element Yagi first director serves both as a secondary driver and as a stabilizing director for wide-band operation. From the perspective of the six-element OWA Yagi, the second and third directors provide the relatively close correlation of current values independently of the first director, which also serves as the secondary driver.

Fig 12 presents the current magnitudes (relative to a primary driver value of 1.0) for the second and third directors of the OWA array. Using the left axis as a guide, we find the values almost identical until the curves diverge above 145 MHz. In the upper region of the frequency scan, where the secondary driver dominates, the curves diverge in value but have similar shapes.

The figure also shows the current phase angles for the same two elements (relative to a constant primary-driver value of 0.0°). The parallel nature of the curves can hardly escape detection.

In Fig 13, the raw data in Fig 12 becomes a set of differentials. The ratio of current between director 2 and director 3 becomes a smooth curve, with only small changes in value in the lower half of the frequency range. (Compare this smooth curve to the "dipper-shaped" curve for the current magnitude ratio of director 1 to director 2 in Fig 11 for the five-element beam.) The amount of phase-angle difference change is even more startling—less than 16.5° overall from 139 to 149 MHz. Likewise, compare this value to the 72° change in difference in Fig 11 across the same range for the first and second directors of the five-element array. Indeed, we might categorize the second and third directors of the OWA as "stabilizing" directors.

Achieving the greatest impedance bandwidth from the OWA array appears to require the added element

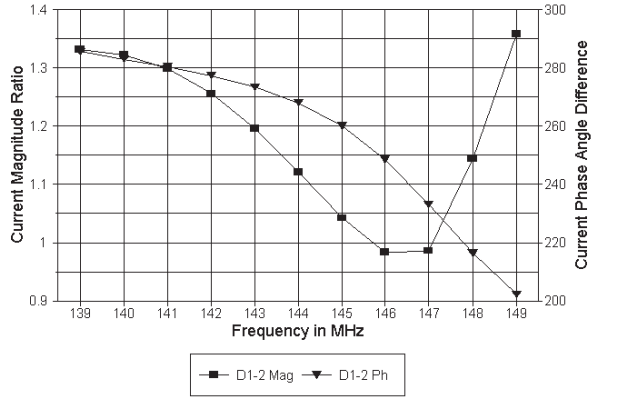

Fig 11—The current-magnitude ratio and the current phase-angle differential between directors 1 and 2 on model 2M5EL16.

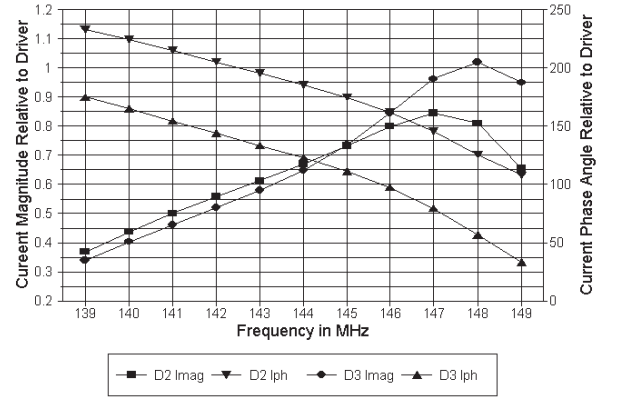

Fig 12—The current magnitudes and phase angles of directors 2 and 3 on model OWA2M616 from 139 to 149 MHz relative to a value of 1.0 and 0.0° on the center segment of the driven element.

within the same boom length in order to arrive at the most stable wide-band operation. Indeed, what sets the OWA design apart from past wide-band parasitic arrays is the combination of a close-spaced secondary driver and the pair of stabilizing directors of equal or very nearly equal length. Closer spacing of the secondary driver permits the achievement of higher median impedance with the same reflector spacing. Since one needs an added director to fill the void in order to reach performance specifications for a given boom length, the new director and the next together—when properly set in length and spacing—complete the broadbanding design operation. Indeed, the impedance bandwidth of the OWA Yagi tends to decrease as the second and third directors diverge in length for a given spacing. In short, it is the entire array design—or at least the first five elements of it—that marks out an OWA Yagi from wide-band Yagis of the past.

The six-element OWA Yagi used as a comparator so far is only one of many possible designs. It is relatively short, and has a narrow operating passband relative to the impedance passband. Therefore, there is still considerable OWA ground to examine.

Some Additional OWA Benefits

The OWA basic platform consists of the reflector through director 3—at least. In a six-element design, only one director remains to control performance at the band edges (in conjunction with small changes to the reflector length). Achieving a wider operating passband—perhaps one that covers most of the impedance passband—becomes considerably easier with the addition of an extra director or two. Ahead of the basic OWA "cell," we may "stagger" tune the directors to arrive at a very significant operating passband.

For a better test of wide-band performance potential, we may move our discussion to the 420 to 450-MHz band, which has a bandwidth that is nearly 7% of the center frequency. Fig 14 presents the outline of a 12-element OWA Yagi that will cover the entire band with reasonable performance. The dimensions for model OWA432E appear in Table 5. Like many Yagis for this band, the array uses 4-mm-diameter aluminum elements. The remaining dimensions appear in both millimeters and wavelengths. At a boom length (minus any extensions) of 2.93 λ, the array is comparable to other 12-element Yagis for this band.

The overall performance of the Yagi is quite adequate for many purposes. The 50-Ω SWR is only 1.5:1 at the band edges. Free-space gain ranges from 13.35 dBi to 14.70 dBi across the band, with a peak near 445 MHz. The 180° and worst-case front-to-back ratios tend to parallel the gain curve, although with a much sharper peak.

The only assessment that we can reach at this stage is that the array is capable of providing service across the entire band. Further assessment requires some sort of standard against which to measure the OWA Yagi. Perhaps the most notable wide-band Yagis for the 420 to 450-MHz band are those developed by Gunter Hoch, DL6WU. His sequence of arrays evolved over two decades of work, with perhaps the last iteration in the RSGB *VHF/UHF DX Book*. Twelve elements is close to the shortest recommended length for a DL6WU array, but it does provide an interesting comparator against which

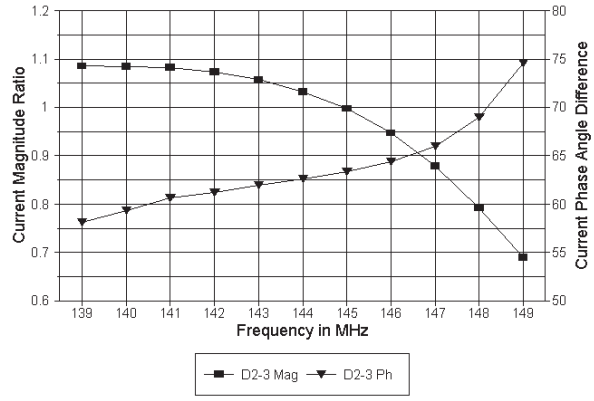

Fig 13—The current-magnitude ratio and the current phase-angle differential between directors 2 and 3 on model OWA2M616.

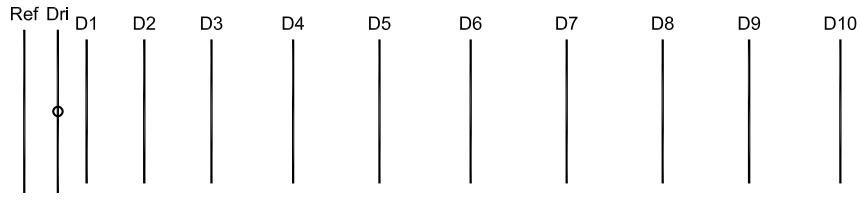

Fig 14—An outline sketch of a 12-element OWA Yagi, showing the traditional element designations. Model OWA432E: see Table 5 for dimensions.

Table 5—Model OWA432E Dimensions

Dimensions of a 12-element 420-450-MHz OWA Yagi, using 0.1575" (4 mm) diameter elements. Wavelength (λ) measurements are for a design center frequency of 435 MHz.

	Length		*Cumulative Spacing*		*Individual Spacing*	
Element	*mm*	*λ*	*mm*	*λ*	*mm*	*λ*
Refl	334.4	0.482	—	—	—	—
Driver	331.0	0.477	106.6	0.154	106.6	0.154
Dir 1	302.0	0.435	149.5	0.215	42.9	0.061
Dir 2	297.4	0.429	244.8	0.353	95.3	0.138
Dir 3	297.4	0.429	377.0	0.543	132.2	0.190
Dir 4	296.4	0.427	550.8	0.794	173.8	0.251
Dir 5	288.2	0.415	762.0	1.098	211.2	0.304
Dir 6	281.0	0.405	1010.3	1.456	248.3	0.358
Dir 7	275.2	0.397	1267.8	1.827	257.5	0.371
Dir 8	269.4	0.388	1535.4	2.213	267.6	0.386
Dir 9	263.6	0.380	1770.5	2.551	235.1	0.338
Dir 10	255.6	0.368	2032.5	2.929	262.0	0.378

to set the OWA design just described.

Fig 15 presents an outline of the DL6WU 12-element Yagi, revealing the operative regularity of element spacing and length used throughout the sequence. Table 6 provides the dimensions, once more using 4-mm elements and presented in terms of millimeters and wavelengths. At 2.85 λ long, the DL6WU array reasonably approximates the boom-length of the OWA Yagi.

The DL6WU arrays all place the driver 0.2 λ ahead of the reflector, with the first director spaced 0.075 λ further forward. This combination—suited to the 4-mm elements—warrants the label "wide-band" to a very high degree. Fig 16 overlays the 50-Ω SWR curves for both the OWA and the DL6WU Yagis between 415 and 455 MHz. The extended range illustrates the "reserve" bandwidth provided by the DL6WU array, compared to the relative tightness of the fit between the band limits and the OWA SWR curve. More significant is that the DL6WU SWR curve shows three minima, compared to the standard two for the OWA.

The SWR curves are related to the progression of the relative current magnitude on the first directors of the respective arrays. In Fig 17, the OWA curve hovers just under a relative magnitude (to a driver value of 1.0) of 0.9. Then, at about 442 MHz, the director current magnitude surpasses that of the driver for the remainder of the operating passband. In contrast, the DL6WU curve rises above a value of 1.0 in two places. The rise and fall of the first director's relative current magnitude correlates also to SWR maximums and minimums.

These and other performance figures for the DL6WU and OWA models appear in Table 7. For the record, Fig 18 compares the free-space gain of the two antenna models. The DL6WU version reaches a peak gain about one-quarter decibel higher than the OWA model, but the OWA gain falls off more slowly at the high end of the band. The gain differential between minimum and maximum is over 1 dB for both arrays.

The OWA array shows a single peak in its 180° front-to-back performance, as indicated clearly by Fig 19. In contrast, the DL6WU array shows two maximums, one slightly below the lower end of the band and the other slightly higher in frequency than the gain peak. The twin front-to-back peaks are related to the number of directors in the array. As one adds directors according to the DL6WU scheme, the front-to-back peaks move upward in frequency. At a certain point, a new low-end peak emerges and the remaining peaks are closer together in frequency. A 26-element array has three front-to-back peaks. The proximity of peaks in turn limits the amount that

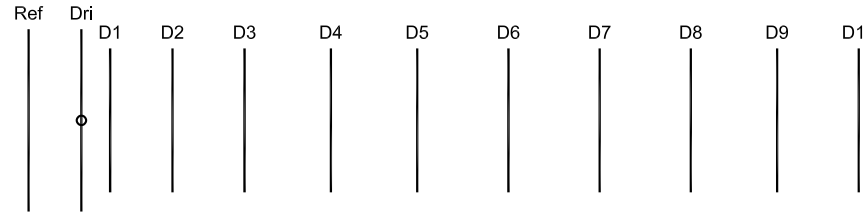

Fig 15—An outline sketch of a 12-element DL6WU Yagi, showing the traditional element designations. Model DL6WU12: see Table 6 for dimensions.

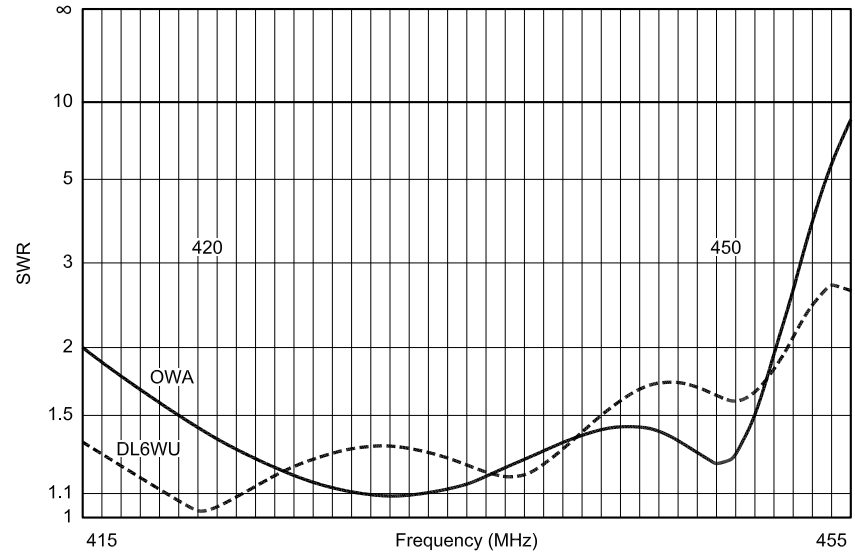

Fig 16—Comparative 50-Ω SWR curves from 415 to 455 MHz for models OWA432E and DL6WU12.

Table 6—Model DL6WU12 Dimensions

Dimensions of a 12-element 420-450-MHz DL6WU Yagi using 0.1575" (4 mm) diameter elements. Wavelength (λ) measurements are for a design center frequency of 432 MHz. Dimensions are adapted from Chapter 10 of *The VHF/UHF DX Book*, from RSGB.

	Length		*Cumulative Spacing*		*Individual Spacing*	
Element	*mm*	*λ*	*mm*	*λ*	*mm*	*λ*
Refl	340.6	0.491	—	—	—	—
Driver	330.0	0.476	138.8	0.200	138.8	0.200
Dir 1	301.6	0.435	190.8	0.275	52.0	0.075
Dir 2	299.2	0.431	315.8	0.455	125.0	0.180
Dir 3	295.6	0.426	465.0	0.670	149.2	0.215
Dir 4	292.2	0.421	638.4	0.920	173.4	0.250
Dir 5	289.2	0.417	832.8	1.200	194.4	0.280
Dir 6	286.4	0.413	1040.9	1.500	208.1	0.300
Dir 7	284.2	0.410	1259.5	1.815	218.6	0.315
Dir 8	282.2	0.407	1488.6	2.145	229.1	0.330
Dir 9	280.4	0.404	1728.0	2.490	239.4	0.335
Dir 10	278.8	0.402	1977.8	2.850	249.8	0.360

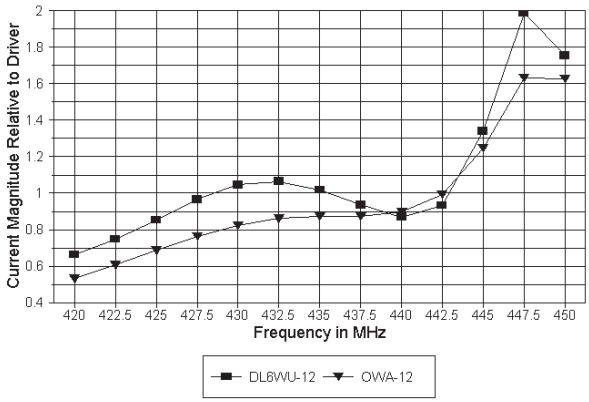

Fig 17—Comparative curves of the relative current magnitude on Director 1 of models OWA432E and DL6WU12, where the primary driver current magnitude is always 1.0.

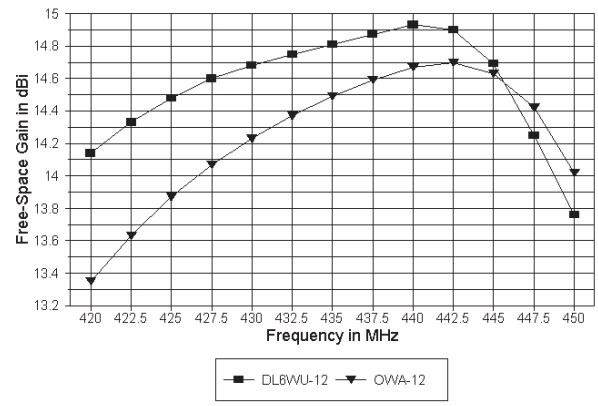

Fig 18—Comparative curves of free-space array gain for models OWA432E and DL6WU12 from 420 to 450 MHz.

the front-to-back value can decrease between peaks. Hence, very long DL6WU Yagis tend to have high minimum front-to-back values.

In terms of SWR bandwidth, gain and possibly front-to-back performance, the DL6WU 12-element array tends to outperform the OWA Yagi. At the present stage of development, it is not clear that the OWA design has reached the limits of its performance. Many folks view the first director in HF OWA Yagis as an added element. Thus, a six-element 20-meter OWA is comparable in length and performance to a standard five-element 20-meter Yagi, both with boom-lengths near 48 feet. However, the OWA design used in the example that we have explored extends the element spacing so that the 12-element boom-length is comparable to that of a standard—or at least a DL6WU—design. Whether element spacing compression to add an 11th director in the same boom length, with appropriate setting of element lengths, can broaden the SWR curve and/or increase the basic gain and front-to-back values across the band remains for further design efforts.

There is one department, little recognized by many Yagi builders, in which the OWA Yagi shows superiority over almost all other Yagi designs of comparable length. Fig 20 illustrates the region of concern with a set of free-space azimuth (E-plane) patterns taken at selected frequencies across the band. Numerical data appear in Table 7. DL6WU himself registers the forward side-lobe strength of his designs as about 17 dB. The 12-element version of his array shows slightly better figures up until the region of highest gain. From about 440 MHz upward, the first forward side lobe becomes so wide that it merges with the main forward lobe. The result is a "bulge" in the main forward lobe, since the pattern cannot show a depression by which most computer model programs would recognize a new lobe. In Table 7, the bulge for the first forward lobe is almost invisible (in the –12-dB region), leaving one with a value for the forward side lobe that actually applies to the second lobe.

Table 7—Comparative Performance Data: OWA2M126A and DL6WU-12

Comparative 420-450-MHz performance data from models OWA432E and DL6WU12. See text for discussion.

OWA12M126A

Frequency (MHz)	*420*	*427.5*	*435*	*442.5*	*450*
Free Space Gain (dBi)	13.35	14.07	14.49	14.70	14.02
180° F/B (dB)	16.36	17.58	18.16	25.28	22.47
Worst-Case F/B (dB)	16.36	17.58	18.16	23.48	20.21
Fwd/Fwd Side Lobe (dB)	21.24	23.03	24.82	26.87	22.42
–3 dB Beamwidth (°)	40.2	38.4	35.0	35.0	34.2
Feedpoint R (Ω)	33.41	44.86	44.58	46.38	39.05
Feedpoint X (Ω)	–2.68	3.16	3.23	16.98	–14.23
SWR (50 Ω)	1.504	1.136	1.143	1.431	1.497

DL6WU-12

Frequency (MHz)	*420*	*427.5*	*435*	*442.5*	*450*
Free Space Gain (dBi)	14.14	14.60	14.81	14.90	13.76
180° F/B (dB)	24.47	17.26	15.53	21.40	16.11
Worst-Case F/B (dB)	20.83	17.26	15.53	21.40	16.11
Fwd/Fwd Side Lobe (dB)	18.21	18.12	17.36	15.74*	19.78*
–3 dB Beamwidth (°)	37.2	35.0	33.0	31.4	30.8
Feedpoint R (Ω)	48.39	63.76	50.23	46.93	39.87
Feedpoint X (Ω)	–2.75	–1.96	–10.44	21.30	–19.85
SWR (50 Ω)	1.067	1.278	1.231	1.554	1.639

*signals the existence of a main-forward-lobe bulge rather than a true side lobe with an intervening pattern depression.

Strong forward side lobes have an interesting consequence beyond radiating power in directions other than the desired one. They also tend to narrow the half-power beam width significantly, perhaps by as much as 3° or nearly 10% of the 30 to 35° beamwidth for these arrays.

In contrast to the strong forward side lobes of the DL6WU array (and many others used in the 420-450-MHz band), the OWA Yagi exhibits a forward side lobe value averaging about

23.7 dB down from the main lobe. The result is a main forward lobe about 3° wider than that of the DL6WU beam. Over narrower operating regions, the OWA Yagi is capable of even better horizontal (E-plane) forward side-lobe suppression. The quest for such suppression does not itself address the equally important question of vertical or H-plane side-lobe suppression.

A second advantage offered by the OWA structure is that it offers a stable basic platform for the development of families of Yagis. The DL6WU Yagi family is perhaps most familiar to builders of VHF and UHF arrays, since the builder can select a boom length and—with reference to a chart provided by DL6WU—the appropriate number, length and spacing of elements to fill the boom. For any boom length above about eight elements, the impedance performance of the array will be similar with almost any number of directors.

Table 8 provides the dimensions of a seven-element, two-meter OWA Yagi that is quite capable of forming the basic unit for a family of two-meter OWA Yagis. The outline appears in Fig 21. The design improves upon the six-element OWA—itself a perfectly good antenna—by optimizing the ele-

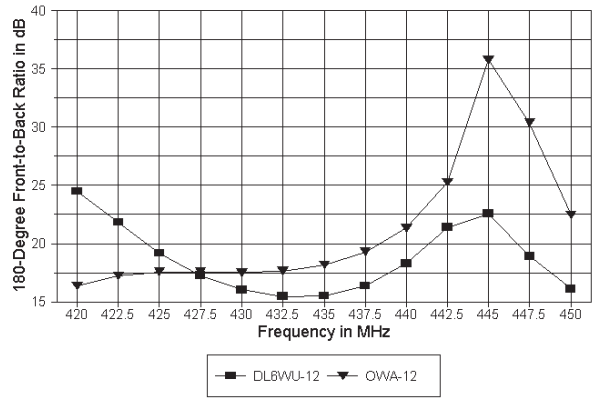

Fig 19—Comparative 180° front-to-back ratio curves for models OWA432E and DL6WU12 from 420 to 450 MHz.

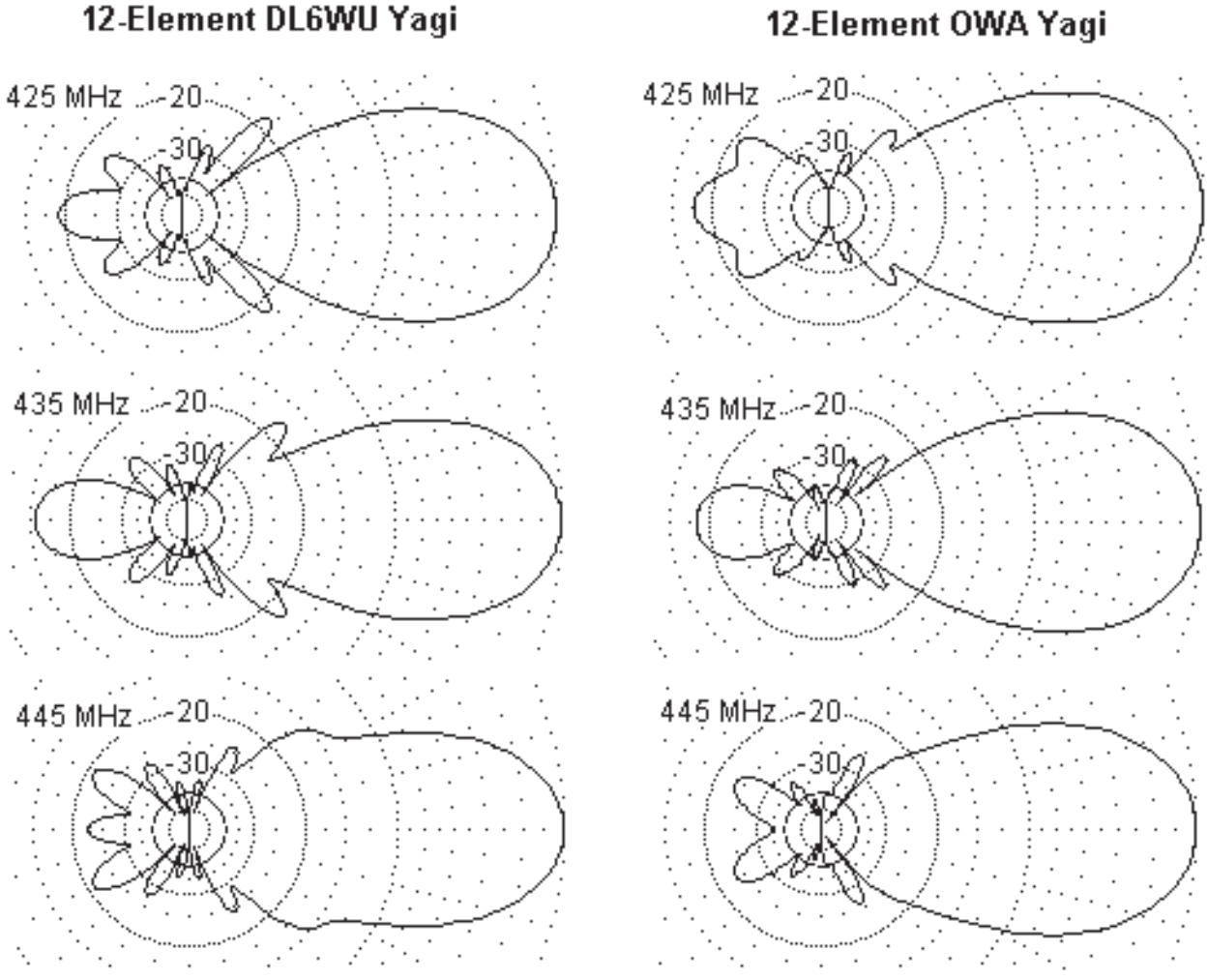

Fig 20—Comparative free-space azimuth (E-plane) patterns of models OWA432E and DL6WU12 at 425, 435 and 445 MHz, with special focus on the forward side-lobe structure and the horizontal –3-dB beamwidth. See Table 7 for numeric data.

ment spacing for the 3/16-inch elements. Since these elements are larger in diameter when measured in wavelengths than the HF arrays upon which the VHF designs are based, wider element spacing goes some distance in optimizing the mutual coupling between elements. Compare the dimensions to those in Table 1 for the six-element array.

Table 9 supplies the complete performance and current data for the model, again inviting a comparison with Table 2, the same data for the original six-element OWA Yagi. Fig 22 samples the data by showing the free-space gain and the 180° front-to-back ratio of the larger beam across the scanned frequency range. Across the operating range from 144 to 148 MHz, the gain varies by less than a one-quarter decibel, from a low of 11.37 dBi to a high of 11.6 dBi for a boom length of 1.06 λ. The 180° and worst-case front-to-back ratios exceed 20 dB across the same range.

More significant for the moment is that the seven-element OWA Yagi is the basis for a family of OWA Yagis ranging from 7 to 12 elements.

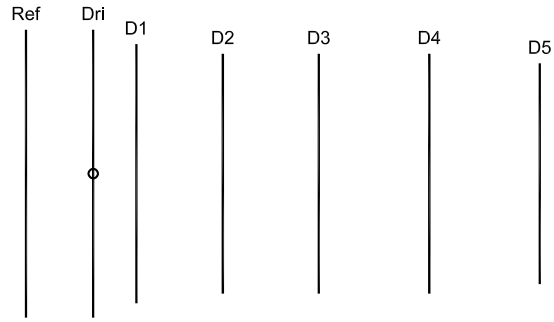

Fig 21—An outline sketch of a seven-element OWA Yagi, showing the traditional element designations. Model OWA2M716A: see Table 8 for dimensions.

Table 8—Model OWA2M716A Dimensions

Dimensions of a 7-element 2-meter OWA Yagi, using 0.1875" (3/16") diameter elements. Wavelength (λ) measurements are for a design center frequency of 146 MHz.

	Length		*Cumulative Spacing*		*Individual Spacing*	
Element	*inches*	*λ*	*inches*	*λ*	*inches*	*λ*
Refl	40.70	0.504	—	—	—	—
Driver	39.66	0.491	10.81	0.134	10.81	0.124
Dir 1	37.00	0.458	15.47	0.191	4.66	0.057
Dir 2	36.32	0.449	27.38	0.339	11.91	0.148
Dir 3	36.32	0.449	42.72	0.529	15.34	0.190
Dir 4	36.20	0.448	63.38	0.784	20.66	0.255
Dir 5	34.50	0.427	85.67	1.060	22.28	0.276

Table 9—7-Element 2-Meter OWA Yagi

NEC-4 reported performance data for model OWA2M716A from 139 to 149 MHz. Current data consist of the relative current magnitude and phase angle on the center segment of each element, where the driver current magnitude is always 1.0 and the driver phase angle is always 0.0°. The "D2 versus D3 Currents" data consist of the ratio of current magnitude from Director 2 to Director 3 and of the current phase angle difference between the two directors. (See text for data interpretation.)

Performance											
Frequency (MHz)	*139*	*140*	*141*	*142*	*143*	*144*	*145*	*146*	*147*	*148*	*149*
Free Space Gain (dBi)	10.75	11	11.17	11.29	11.4	11.5	11.58	11.61	11.56	11.37	10.99
180° F/B (dB)	11.02	12.86	14.58	16.33	18.35	21.05	25.03	28.73	24.68	20.37	18.11
R (Ω)	30.89	36.35	40.81	43.62	44.94	45.7	47.3	51.01	55.07	46.97	25.4
X (Ω)	–10.72	–6.21	–3.47	–1.62	0.46	3.41	6.92	8.952	4.47	–6.87	–3.62
SWR (50 Ω)	1.734	1.419	1.242	1.151	1.113	1.122	1.165	1.195	1.137	1.167	1.982
Currents											
Ref-Magnitude	0.776	0.739	0.685	0.621	0.557	0.505	0.472	0.458	0.438	0.344	0.169
REF-Phase (°)	144.28	135.41	127.16	120.13	114.78	110.99	107.63	101.98	89.74	69.2	54.97
D1-Magnitude	0.49	0.582	0.667	0.738	0.798	0.859	0.946	1.098	1.339	1.514	1.359
D1-Phase (°)	–76.13	–81.3	–87.23	–93.04	–97.94	–101.5	–103.9	–106.9	–115	–132.2	–150.5
D2-Magnitude	0.396	0.463	0.526	0.585	0.639	0.692	0.752	0.819	0.865	0.783	0.611
D2-Phase (°)	231.5	223.6	215	206.1	197.3	188.7	179.79	169.31	155.34	139.86	139.76
D3-Magnitude	0.399	0.464	0.526	0.582	0.637	0.7	0.79	0.934	1.144	1.299	1.234
D3-Phase (°)	156.31	145.99	135.17	124.45	114.33	104.9	95.57	84.54	68.13	43.8	20.21
D4-Magnitude	0.365	0.437	0.509	0.58	0.653	0.737	0.847	1.002	1.194	1.271	1.085
D4-Phase (°)	65.02	52.36	38.78	24.77	10.62	–3.76	–19.15	–37.43	–62.18	–95.43	–127.8
D5-Magnitude	0.256	0.302	0.346	0.387	0.425	0.467	0.519	0.59	0.671	0.675	0.539
D5-Phase (°)	–40.82	–55.52	–71.18	–87.34	–103.7	–120.3	–138	–158.7	174.17	138.53	103.75
D2 versus D3 Currents											
Magnitude Ratio	0.992	0.998	1	1.005	1.003	0.989	0.952	0.877	0.756	0.602	0.495
Phase Difference (°)	75.19	77.61	80.23	81.65	82.97	83.8	84.22	84.77	87.21	96.06	119.55

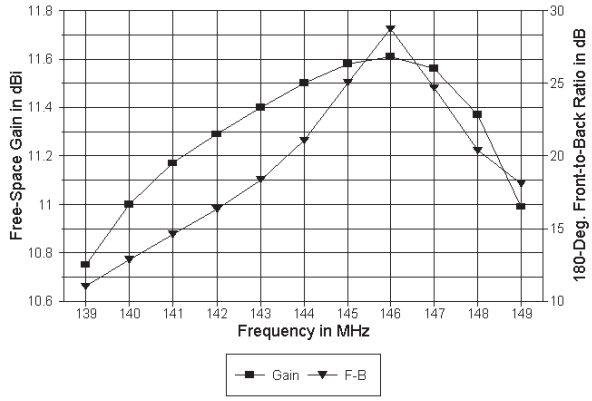

Fig 22—The modeled free-space gain and 180° front-to-back performance of Model OWA2M716A from 139 to 149 MHz. See Table 9 for numeric data.

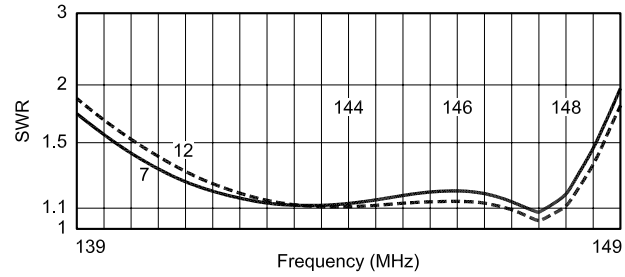

Fig 23—50-Ω SWR curves for model OWA2M716A and OWA2M126A from 139 to 149 MHz.

However, the design requirements for increasing the number of elements vary from those applicable to the simple scheme of a typical DL6WU design. For each additional element, the designer must reset the length and spacing of the former forward-most element to establish it in its new role as next to the most forward element. This step enables the designer to replicate the impedance curve and the shape of the performance curves for the larger array. The final step is setting the length and spacing of the new forward-most element to set the band-edge performance.

Table 10 presents the dimensions of a 12-element OWA Yagi that is the outgrowth of applying the procedure just given. The outline of the array is the same as for the 12-element 420-450-MHz array in Fig 14. The first six elements are identical to those in the seven-element array. The seventh element (fifth director) changed length and spacing, growing in both departments, as it entered the eight-element member of the family.

Fig 23 provides 50-Ω SWR scans for both the 7- and 12-element members of the OWA 20-meter family, using the 139 to 149-MHz sweep with which we started. The scans testify to the stability of the OWA core to support long-boom Yagis while maintaining easily controlled impedance conditions. The performance curves for the 12-element OWA Yagi resemble those for the seven-element cousin, but at a higher gain level. Performance data appears in Table 11. Within the 144 to 148-MHz operating range, the free-space gain averages 14.3 dBi, with a 0.34 dB variation across the band. The lowest worst-case front-to-back ratio is 22.9 dB, with the highest front-to-back ratio only 1.7 dB higher. In short, performance is very even across the band.

As significant is the forward side-lobe suppression figure, which averages 26.3 dB across the two-meter band. Since the worst-case front-to-back ratio is in almost all cases related directly to the main rear lobe, there appears to be a secondary effect, namely, some reduction in the side lobes in the rear quadrants.

Table 10—Model OWA2M126A Dimensions

Dimensions of a 12-element 2-meter OWA Yagi, using 0.1875" ($^3/_{16}$") diameter elements. Wavelength (λ) measurements are for a design center frequency of 146 MHz.

	Length		*Cumulative Spacing*		*Individual Spacing*	
Element	*inches*	*λ*	*inches*	*λ*	*inches*	*λ*
Refl	40.70	0.504	—	—	—	—
Driver	39.66	0.491	10.81	0.134	10.81	0.124
Dir 1	37.00	0.458	15.47	0.191	4.66	0.057
Dir 2	36.32	0.449	27.38	0.339	11.91	0.148
Dir 3	36.32	0.449	42.72	0.529	15.34	0.190
Dir 4	36.20	0.448	63.38	0.784	20.66	0.255
Dir 5	35.20	0.435	88.85	1.095	25.47	0.311
Dir 6	34.30	0.424	118.0	1.460	29.15	0.365
Dir 7	33.60	0.416	148.6	1.838	30.60	0.378
Dir 8	32.90	0.407	180.4	2.232	31.80	0.394
Dir 9	32.20	0.398	212.0	2.622	31.60	0.390
Dir 10	31.20	0.386	240.0	2.969	28.00	0.347

Table 11—Modeled Performance Data: OWA2M126A

2-meter performance data from model OWA2M126A.

Frequency (MHz)	*144*	*145*	*146*	*147*	*148*
Free Space Gain (dBi)	14.10	14.27	14.40	14.44	14.30
180° F/B (dB)	22.90	23.76	24.63	24.65	22.97
Worst-Case F/B (dB)	22.90	23.76	24.60	24.37	22.97
Fwd/Fwd Side Lobe (dB)	25.16	26.69	27.92	26.67	25.06
Feedpoint R (Ω)	48.61	50.22	51.79	53.01	47.49
Feedpoint X (Ω)	4.98	6.07	6.43	3.70	–4.36
SWR (50 Ω)	1.111	1.129	1.140	1.097	1.109

Conclusion

If the concept of an optimized broadband antenna (OWA) refers only to the arrangement of the reflector, driver and first director, then there is little to distinguish it from past attempts to achieve wide-band performance. The one possible exception is the closer than usual spacing between the driver and the first director. However, this close spacing does not affect the role of the first director as a secondary or parasitic driver for the array.

In contrast, treating the OWA concept as including all array elements at least through the third director opens the way to appreciating more fully the potentials of this Yagi arrangement. The relative stability of the current ratio and phase-angle difference between the second and third directors tends to permit increased impedance bandwidth with lower levels of variation. In combination with the reflector-driver-first-director arrangement, the entire assembly offers excellent control over the feed-point impedance throughout at least a 7% overall bandwidth, with greater bandwidths possible.

Although OWA Yagi arrangements often have operational passbands that cover only part of the impedance passband, it is possible to design Yagis for nearly full impedance passband coverage, although present designs have lower average performance than those using only a portion of the impedance passband. As well, the OWA arrangement holds potential to form the basis for families of long-boom Yagis with only slight reductions in gain relative to gain-oriented designs. However, the OWA designs offer superior front-to-back performance and greater suppression of forward side lobes than most extant Yagi designs.

The OWA Yagi arose from experimental results using computerized optimizing routines. To date, amateur literature has not seen a full analysis of how the OWA acquires its interesting properties relative to other Yagi designs. These notes are but a partial contribution in the direction of more fully understanding the OWA Yagi. As others develop understandings to supplant this one, it is very likely that the proof-of-principle designs used as examples in these notes will also be supplanted by far more capable Yagi arrays. □□